Microfluidic cell-chip for an *in vitro* hepatic disease model

Sofia Alves Bernardo Pirata Relvas
sofia.relvas@tecnico.ulisboa.pt
Universidade de Lisboa, Instituto Superior Técnico, Lisbon, Portugal
November 2021

Abstract

Hepatocytes and Kupffer cells (KCs) are involved in insulin resistance (IR) disease. However, the impact of KCs on hepatocyte's pathological phenotype still needs to be further investigated with the view to achieve new therapies. To do that, more physiologically relevant hepatic *in vitro* models are required. Microfluidic devices have an enormous potential to develop this type of models, providing a better mimicking of the liver environment than macroscopic cultures. Here, a microfluidic device to in the future study the interactions between hepatocytes and KCs was designed and fabricated. As the device is complex, we only focused on adapting and characterizing hepatocytes in it. Stem cell-derived hepatocyte-like cells (HLCs) were employed in this work since they demonstrated to be a promising alternative for the development of hepatic models.

A two layer hepatocyte-chip was successfully fabricated. Optimizations were firstly performed with the view of fully adapt the HLCs culture into their chamber. The maintenance of HLCs for more than one week into the chip was accomplish, having presented polygonal morphology. To demonstrate that the chip can provide off-the-shelf models, adaptation of cryopreserved HLCs was accessed. Fresh and cryopreserved HLCs demonstrated higher urea production comparing with HLCs cultured in regular plates, proving the potential of microscale cultures.

In conclusion, the work here accomplished constitutes the first step towards the development of an *in vitro* hepatic model intended to integrate both hepatocytes and KCs to be used in disease modelling and drug testing studies.

Keywords – Microfluidic device; Liver; Hepatocyte-like cells.

I. Introduction

I.1. Overview of liver structure and functions

The liver is a large organ that is located in the upper-right part of the abdominal cavity [1]. Blood is supplied to the liver by two main sources: the portal venule, which contains blood rich in nutrients, and the portal arteriole, where oxygenated blood flows [1]. The liver is organized into hexagonal-shaped lobules [2]. Each lobule has in its constitution the central vein that is located in the middle part of the hexagon [3]. In the corners, there is the portal triad constituted by the portal venule, the portal arteriole, and the bile duct [2]. The foundations of the lobules are composed of the hepatocytes, which are parenchymal cells and represent 60% of the total number of hepatic cells [2].

Hepatocytes are subjected to two types of flow, the blood flow in its basolateral membrane and a bile flow in its apical membrane, conferring to these cells the particularity of being highly polarized [4]. The two blood supplies of the lobule drain blood to the central vein through the sinusoids [2]. Between the sinusoids and the hepatocyte's basolateral membrane, there is the space of Disse, which is composed of an extracellular matrix that offers support and structure to the hepatocytes [2]. The space of Disse also contains hepatocyte's microvilli that have the important role of communicating with the blood supply [2]. Also inside the lobule, bile canaliculi are formed by the hepatocyte's apical membranes, which facilitate the bile flow towards the bile duct [2].

Besides hepatocytes, the liver is also composed of non-parenchymal cells namely Kupffer cells (KCs). KCs are the liver macrophages that are localized in the inner side of the sinusoids adherent to the endothelial cells [5]. These cells, which constitute 12% of the total hepatic cell's number, protect the liver from bacterial infections and toxic agents [6].

The liver is the main organ that governs the energy metabolism in our body [7]. The blood that comes from the digestive tract is filtered by the liver which captures the nutrients and uses them in several metabolic pathways [8]. By them, the liver maintains the blood glucose levels, degrades and produces lipids according to the energy demand, but also stores them in other tissues, and synthesizes ketone bodies, which are an important intervenient in brain energy generation during starvation [7]. The liver is the major handler of protein metabolism as it produces blood proteins that transport substances to other organs [7]. Furthermore, it is also involved in the urea metabolism, metabolizes drugs into nontoxic substances, and it is involved in the production of bile [9].

I.2. Liver's role in insulin resistance

IR occurs due to a decrease in both peripheral tissues and hepatocytes' metabolic response to insulin [10]. Consequently, higher concentrations of this pancreatic hormone are needed to achieve a normal metabolism [10].

IR is considered as a subsequent cause of obesity [10]. The western diet is considered the major booster of obesity since it is highly rich in fat and sugar [11]. These diets lead to augmented visceral fat, which will increase the quantity of free fatty acids (FFAs), cytokines and pro-inflammatory substances in the portal circulation (Figure 1) [12]. That will trigger lipid accumulation in hepatocytes which will impair the glucose uptake induced by insulin, reducing the hepatocyte's sensitivity to that hormone. Therefore, insulin fails to inhibit hepatic gluconeogenesis and glycogenolysis, which leads to high glucose concentrations in

the blood, and, consequently, compensatory insulin production and secretion by the pancreas, leading to hyperinsulinemia [13]. Hyperglycemia and hyperinsulinemia contribute to the maintenance of fatty acids' synthesis [6]. Advances in this condition lead to KCs activation to a pro-inflammatory phenotype amplifying the hepatic inflammatory state and further contributing to insulin sensitivity [14].

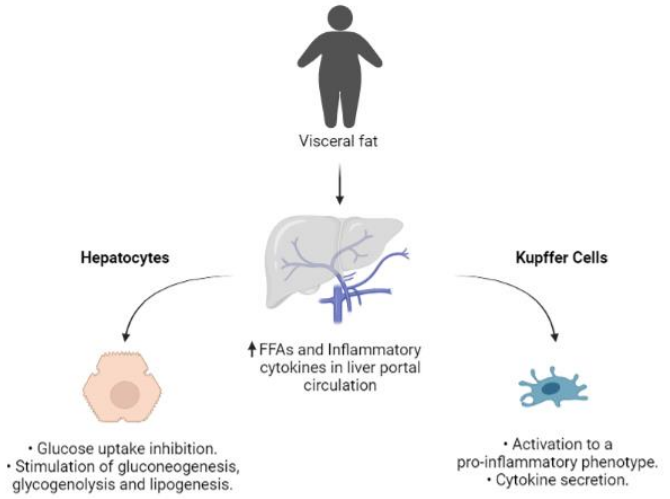

Figure 1- Development of insulin resistance: the effects on hepatocytes and Kupffer cells functions.

I.3. Deriving hepatocytes to create human in vitro hepatic models

Stem cells (SCs) have a great potential to originate mature hepatocytes in large amounts due to their ability to self-renewal [15]. By offering advantages over other SC types, mesenchymal stem cells (MSCs) may be regarded as a promising alternative for the development of *in vitro* platforms for toxicological assessment, disease modeling, and drug screening. MSCs from the human neonatal umbilical cord tissue (hnMSCs-UCM) seem to be one of the most advantageous primary sources since they are strongly available, easy to expand *in vitro* and, come from a tissue that would be discarded otherwise [16]. hnMSCs-UCM are able to be differentiated into HLCs by the mimicking of the liver embryogenesis [15]. Cipriano *et al.* described an optimized protocol to generate mature HLCs through hnMSCs-UCM with a phenotype closer to the primary human hepatocytes (hpHeps) than HepG2 (tumor cell line) [17]. Besides, through that protocol, HLCs could be successfully maintained in culture up to 34 days without losing hepatic functions [17].

I.4. Microfluidic Devices

Microfluidics is defined as being the science and technology behind systems that are built to manipulate or process fluids on the microscale level [18]. These systems are often characterized as microfluidic devices with critical dimensions [19].

Advantages of the microfluidic systems over the conventional macroscale systems are their portability, the improved temperature control, and analytical sensitivity [20]. They have the possibility of being easily actuated by valves and pumps integrated inside them, and manipulated through the use of syringes and pumps outside [20]. Moreover, they can also be embedded in other systems, and are designed according to the goal of the study [20].

The microfluidic device's fabrication is mostly carried out by polydimethylsiloxane (PDMS), which is optically transparent, soft, and compatible with cell culturing [21]. Its capability to support widely used components of the microsystems, such as valves, pumps, and mixers, makes it a great material for microfluidic research [21].

I.5. Microtechnology in biological applications

The small size of the microfluidic devices plays an important role when it comes to the manipulation of living tissues and cells [18]. This makes the experimental costs, reagent volumes, and cell number needed small, enabling precise microenvironment control [22]. In microfluidic devices, only exists diffusion, like in the natural cell's environment [23]. Physiological levels are easier to achieve, since medium-to-cell ratios inside the device are closer to the optimal ones, therefore, avoiding the dilution and ineffectiveness of several molecules and metabolites secreted by the cells, as it happens in culture plates [22]. These devices have also the advantage of being properly designed in order to have the features and geometries that better simulate the desired biological environment [23]. They have the possibility of being operated by perfusion or recirculation and the flow can be unidirectional or bidirectional, which can be acquired to enable a better approximation of the desired system. This technology has, thus, the potential to model biological systems that can be used in pharmacological studies.

I.6. Hepatic cell-chips

By making use of microfluidic devices, it is possible to develop hepatic systems that are shown to be advantageous in comparison to other models used in pharmaceutical research to recreate the human liver.

Microfluidic devices allow the generation of flow-based systems, meaning that the culture medium is circulating within the cells continually, eliminating all metabolites and supplying the cells with nutrients [22]. The imposition of culture medium flow in direction and rate have a great impact on the hepatocyte's phenotype since it simulates blood capillaries [22]. This exerts an influence on the spatial arrangement of the hepatocytes by enabling the maintenance of cell's polarity and tissue-specific activity [22]. Furthermore, it was observed that culturing high-density hepatocytes in a low volume system increase the accumulation of cytokines, increased albumin production, stimulates the formation of bile canaliculi, and the expression of genes involved in the metabolic functions, which approximates these systems to the physiological pattern [22]. In microfluidic devices, hepatocytes can be tightly packed, which allows a stronger cell-to-cell contact, a continuous nutrient exchange, the establishment of a defined tissue and fluid transport regions [22].

Microfluidic devices are, thus, strong instruments to produce interactive, controlled, and reliable *in vitro* human liver models that can be employed in disease modeling and toxicity testing [24].

I.7. Motivation and objectives

Considering that there is lack of liver models to study hepatic IR and it is still needed to understand the mechanisms behind hepatocytes and KCs behavior on this disorder, a microfluidic device, that aimed containing these two hepatic cells, was projected with the objective to *in vitro* create a hepatic IR model (Figure 2). Since the proposed microfluidic device is complex and presupposes the culture of two cell types, it was required to divide its conception into different parts: the hepatocyte culture chamber and its culture medium reservoir (hepatocyte unit), and the Kupffer cell culture chamber and its respective culture

medium reservoir (Kupffer unit). This thesis aims at design the hepatocyte unit of these device and adapt HLCs to it, with the view to, hereafter, create an *in vitro* hepatic model to study the IR mechanisms and the effects of the interactions between hepatocytes and Kupffer cells on the disease progression.

Therefore, the first goal was to make use of microtechnology to design and fabricate a functional hepatocyte unit, the called hepatocyte-chip. The hepatocyte-chip would be composed of two different layers: a fluidic layer, where the hepatocytes will be cultured and the culture medium will flow, and a control layer, where the pneumatic valves will be constructed. The second goal was to adapt HLCs into the designed fluidic layer part of the hepatocyte-chip. The final goal of this work was to prove the workability of the control layer of the hepatocyte-chip through primary actuation tests.

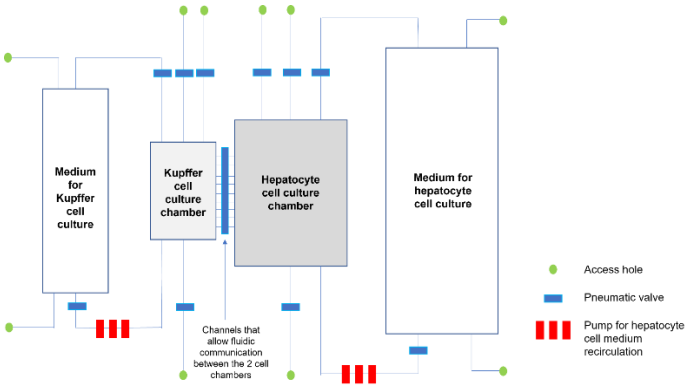

Figure 2- Scheme of the future microfluidic device that will be used to study IR mechanisms regarding the communication of hepatocytes and Kupffer cells.

II. Material and Methods

II.1. Hepatocyte-chip fabrication

II.1.1. AutoCAD® design and hard mask fabrication

The design of the device was done using the AutoCAD® software (Autodesk Inc.). Then, two hard masks were fabricated to create the fluidic layer device, one regarding the chambers and other the channels. And another hard mark had to be done for the control layer. Therefore, the procedures below were performed three times.

A 5x5 cm glass substrate (Coring Inc.) was cleaned using isopropanol (IPA), and deionized water (DI water) followed by an ultrasound bath in Alconox (Alconox Inc.) for 30 minutes at 65ºC. The glass was rinsed with DI water again and dried with compressed air. Aluminum (Al) was deposited on top of the glass surface using the Nordiko 7000 Magnetron Sputterer system (Nordiko Technical Services Ltd.), giving origin to an Al substrate. The deposition of a positive photoresist (JSR) in the Al substrate was done on a swivel plate at 2000 rpm for 1 minute (SVG resist coater Silicon Valley Group Inc.). Next, the wafer was poured on a hot plate at 85ºC for 1 minute to evaporate the photoresist's solvent.

The wafer was placed inside the DWL (Direct Write Lithography System; Heidelberg Instruments). The machine reads the information about the drawing lines and exposes the photoresist leading to its detachment. Afterward, the substrate was heated at 110ºC for 1 minute. After cooling down for 30 seconds, it was washed with a regulator and water (Silicon Valley Group Inc.), to take off the photoresist exposed, while the wafer was spinning on a swivel plate. After that, the aluminum non-covered by the photoresist was removed using an Al etchant (Microchemicals). Finally, the remaining positive photoresist was washed with acetone, IPA, and DI water and dried using an air gun.

II.1.3. Master mold fabrication

A total of two master molds were fabricated, one corresponding to the fluidic layer and the other to the control layer. First, a silicon (Si) substrate (University Wafer) was cleaned with IPA and DI water. Then, was dived in Alconox solution inside a Petri dish and placed in a bath with ultrasounds for 15 minutes at 65ºC. After that, the Si substrate was rinsed with DI water and dried with compressed air. Then, it was poured into the UVO Cleaner for 20 minutes. It was rinsed again with DI water and dried with compressed air. The steps described before were done twice, one for each mold.

Fluidic Layer Mold:

To fabricate the chambers of 100 µm of height, SU-8 50 (Microchem Corp.) was placed on top of the Si substrate in the spinner (Laurel Corp.) to perform the spin-coating to acquire a thickness of 100 µm on the substrate. Next, a pre-exposure bake was done on a hot plate at 65ºC for 11.5 minutes. The temperature was increased to 95ºC. When the 95ºC were reached, 34 minutes were counted. Afterward, the substrate with the photoresist on top was cooled down for 1 minute. The chamber hard mask fabricated lately was placed on top of the SU-8 50. Then, it was poured inside the UV-KUB 2 (Kloé SA), and exposed to UV light for 62 seconds with only 30% of the maximum lamp power. A post-exposure bake took place on a hot plate at 65ºC for 1 minute. Then, another heating ramp was done by increasing the temperature to 95ºC without removing the substrate from the hot plate, and 11.5 minutes were counted after the 95ºC were reached. The substrate was cooled down for 2 minutes. The substrate was submerged in a PGMEA solution (Sigma-Aldrich) for 10 minutes with manual agitation until the non-exposed photoresist was entirely removed. Next, it was cleaned with IPA and dried with compressed air. The last step of this procedure was the hard bake on a hot plate at 150ºC for 15 minutes followed by a slow cool down until it reaches 50ºC.

To create the channels of 35 µm it was used AZ40XT-11D (Merck Performance Materials GmbH). The photoresist was poured on top of the Si substrate with the SU8-50 features. Next, the photoresist is spin-coated. The pre-exposure bake was done by placing the substrate on a hot plate at 100ºC, then, ramping up to 125ºC, and baking for 5 minutes when the latter had been reached. After cooling down for 3 minutes, the channels hard mask was poured on top of the Si substrate and the exposure was done for 10 seconds with 100% of the maximum power of the UV lamp. The substrate was cooled down for 3 minutes and it was developed for 5 minutes using a TMAH based developer solution (micro resist technology GmbH) with manual agitation. Then, it was washed with DI water and dried with compressed air. Finally, the hard bake was performed by placing the substrate on a hot plate for 5 minutes at 80ºC, followed by 5 minutes at 100ºC, 15 minutes at 115ºC, and 5 minutes at 125ºC with temperature ramping.

Control Layer Mold:

The control layer mold was fabricated using SU-8 50. The photoresist was spin-coated in order to achieve a height of 50 µm. The pre-exposure bake was done on a hot plate for 6.6 minutes at 65ºC. The temperature was ramped to 95ºC, and the

substrate was left at that temperature for 20 minutes. After cooling down for 1 minute, the hard mask corresponding to the valves was placed above the Si substrate and the exposition was made for 39 seconds with 30% of the maximum power of the UV lamp. The post-exposure bake was performed at 65ºC for 1 minute. Then, the temperature was increased to 95ºC, and the substrate was left for 5.8 minutes. After cooling down for 2 minutes, the substrate was developed with a PGMEA solution for 7 minutes with manual agitation. Then, the substrate was cleaned with IPA and dried with compressed air. Finally, the hard bake was done in the same way as it was for the 100 µm fluidic layer chambers.

II.1.4. PDMS fabrication and sealing

The PDMS was fabricated by mixing curing agent and base in a ratio of 1:10 in a plastic cup (Dow Corning). The cup was placed inside the desiccator for 45 minutes.

Perfusion hepatocyte-chip structure:

The PDMS was poured on top of the fluidic mold. Next, a PMMA (acrylic glass) plate was placed on top of the frame, and springs were poured on the sides to increase the junction. The baking of the PDMS on its mold was done for 1 hour and 30 minutes at a temperature of 70ºC.

The structure was drilled using an 18 ga syringe tip (Instech Laboratories Inc.) in the places designed for the hepatocyte's chamber access holes. Since it was only needed the hepatocyte's chamber part of the device for the chip operation in perfusion, additionally, a top inlet was drilled in a zone above the top dispenser. Similarly, an outlet was drilled in the zone below the bottom dispenser. Plus, it was necessary to interrupt the communication to the culture medium chamber, therefore, it were drilled two holes above the top inlet and below the bottom outlet to be maintained closed while perfusing the hepatocyte's chamber with medium.

The structures were sealed against the polystyrene (PS) of the Petri dishes using an oxygen plasma bonding. The Petri dishes were placed inside the Plasma Cleaner (Harrick Plasm). 5 minutes of high voltage was performed. After that, a solution of 3-Aminopropyltriethoxysilane (Thermo Fisher Scientific) with water was spilled inside the Petri dishes and it was left for 20 minutes. After that time, the Petri dishes were rinsed with DI water and dried with compressed air. The PDMS structures were washed with IPA followed by DI water and dried with compressed air. Then, they were placed inside the Plasma Cleaner. High voltage for 5 minutes was done. After that, the PDMS structures were poured on top of the PS that received the plasma bonding treatment.

Recirculation hepatocyte-chip structure:

To create the complete structure, the control mold was taped to a Petri dish and PDMS was poured on the top of it in order to cover the entire mold. The Petri dish was placed in the oven for 1 hour and 30 minutes at a temperature of 70ºC. Then, the holes were drilled using a 20 ga syringe. In parallel, the fluidic mold was taped to a PMMA plate. A PMMA frame was poured on top and 3 mL of PDMS was spilled on it. Then, the wafer was placed inside the oven and the PDMS was baked for 1 hour at 70ºC.

Afterward, the control and fluidic PDMS structures were sealed against each other. Therefore, after being washed with IPA and DI water and dried with compressed air, both structures were poured into the Plasma Cleaner. High voltage for 1 minute was applied. After taking the structures of the machine, the valves were aligned with the channels, and the control layer was sealed on top of the fluidic layer creating a PDMS stack. The already sealed structure was peeled off the fluidic mold, and the access holes of the fluidic layer PDMS were drilled using an 18 ga syringe. Then, the complete structures were sealed against Petri dishes by following the same protocol used for the perfusion structure.

II.2. Microfluidic device set-up

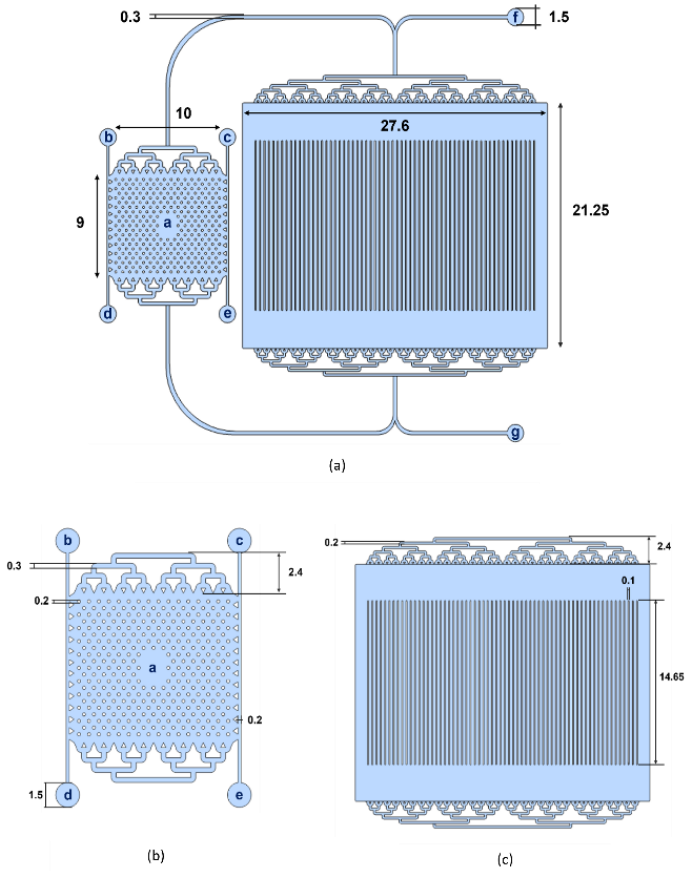

Figure 3- Fluidic layer dimensions of the final hepatocyte-chip in millimeters (mm). In image (a) it is being represented an overview of the main dimensions of the fluidic part of the device. In (b) it is possible to visualize a detailed representation of the cell's chamber including some particular dimensions and the given access hole's nomenclature. Image (c) represents specific dimensions of the culture medium chamber.

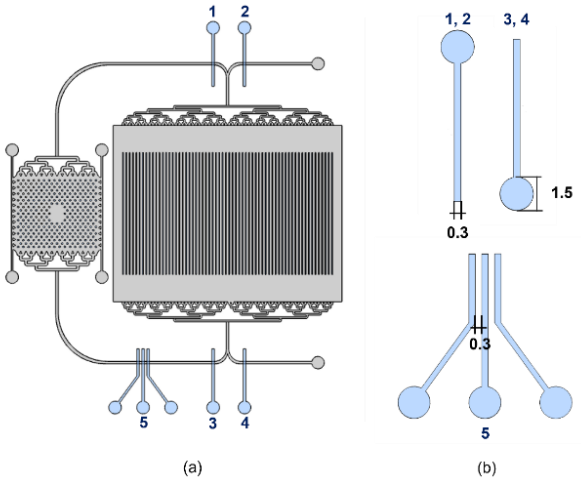

Figure 4- Control layer dimensions of the final hepatocyte-chip in millimeters (mm). In the image (a) it is being represented the disposition of the pneumatic valves and pump throughout the fluidic layer design, and the numbers attributed to each. In (b) it is possible to visualize a detailed representation of each valve conformation and pump, as well as some of their dimensions.

II.3. Reagents for cell culture

All culture media and supplements, solvents and other chemicals were acquired from Sigma-Aldrich unless specified.

II.4. Collagen coating

Rat-tail type I collagen and commercial rat-tail type I collagen (Gibco, UK) were used in this work. The protocol for rat-tail extraction was based on Rajan *et al.* [25]. The extracted rat-tail collagen was dissolved in 0.1% acetic acid to a stock concentration of 1 mg/mL. The stock solution was diluted in PBS to 0.2 mg/mL. After 1 hour of incubation at 37 ºC, cell culture surfaces were washed with PBS before inoculation. The differentiation process occurred using this collagen coating until D17 and onwards for cultures in well plates.

Coating with commercial type I collagen was used for the microfluidic devices. Commercial collagen at a stock concentration of 3 mg/mL was diluted in PBS to a final concentration of 0.2 mg/mL. After 1h in the incubation at 37 ºC, the devices and the well plates were washed with PBS.

II.5. Cell culture

hnMSCs isolated from human umbilical cord stroma were fully characterize and expanded in Eagle's minimum essential medium - alpha modification (α-MEM) supplemented with 10% (v/v) of fetal bovine serum (FBS; Gibco, UK) [26, 27]. A three-step differentiation protocol was applied to hnMSCs [17]. At D17 of differentiation, cells were trypsinized and reinoculated in Iscove's modified Dulbecco's medium (IMDM) with 8 ng/mL oncostatin M (OSM; Peprotech, USA), 1 µM dexamethasone (Dexa), 1% (v/v) DMSO, 1% (v/v) insulin-transferrin-selenium solution (ITS; Gibco, UK), 20 µM of 5-azacytidine (5-AZA), 5% (v/v) FBS, 1% (v/v) penicillin-streptomycin (Pen-strep) and 0.01% (v/v) amphotericin B (Anfo) into (i) microfluidic devices (MDs) and (ii) culture plates pre-coated with collagen. Medium was changed 24h after inoculation to remove 5-AZA and FBS. From D21 onwards, HLCs were maintained in Physiol, composed of Dulbecco's modified Eagle's medium (DMEM) with 1 nM of insulin, 100 nM of Dexa and 0.2% BSA. Medium was replaced every 3 days.

HepG2 cells were cultured in α-MEM supplemented with 10% FBS, 1 mM of sodium pyruvate and 1% (v/v) of non-essential amino acids. Cryopreserved human primary hepatocytes (hpHeps; pool of 10 donors) were purchased from Invitrogen (Carlsbad, USA), thawed on cryopreserved hepatocyte recovery medium (Invitrogen), and manipulated according to manufacturer instructions. Cell cultures of hnMSCs, HepG2 and were maintained at 37 °C in a humidified atmosphere with 5% CO_2 in air. Cell viability was assessed through trypan blue exclusion method.

II.6. Freezing of HLCs

After trypsinization at day 17 of differentiation, HLCs were resuspended in 90% FBS and 10% DMSO and put in cryovials. The vials were placed in an isopropanol cooling container (Mr. Frosty) which was kept at -80 ºC overnight. The vials were then stored in liquid nitrogen until further use.

II.7. Thawing of cryopreserved HLCs

The thawing procedure was performed rapidly using a 37ºC water bath. The aliquots were resuspended in culture medium and centrifuged at 200xg for 5 minutes. HLCs were seeded into (i) microfluidic devices (**Section II.8.3.**) and (ii) culture plates pre-coated with collagen (4×10^4 cells/cm^2) and plated in Diff with 10% FBS and 20 µM of 5-azacytidine. FBS and 5-azacytidine were removed after 24 hours.

II.8. Hepatocyte-chip perfusion assays

The culture medium flowed inside the chamber by making use of a syringe pump (NE-1002C, New Era Pump Systems, Inc., USA) to control the flow rates, syringes (1 mL insulin syringes U-100 Luer-Lock, Codan, DE), 20 ga syringe stubs (Instech Laboratories, Inc., USA), BTPE 60 tube (Instech Laboratories, Inc., USA), and metallic plugs (SC20/15, Instech Laboratories, Inc., USA).

II.8.1. Set-up

The device was submerged in Milli-Q® water to remove the air inside and subjected to 2h of UV exposure inside the laminar flow hood as a sterilization procedure. BTPE 60 tubes were decontaminated with ethanol and then, washed with PBS. Afterwards, the tube was connected to a syringe tip, and a metallic plug was inserted in its other extremity. The syringe tip was attached to a syringe and the syringe poured on a syringe pump. The other tube end was plugged into the device.

II.8.2. Collagen coating

The coating was performed 72h before HLCs inoculation. The collagen solution was flowed inside the device, through inlet **a** (Figure 3a), using 50 µL/min for 2 min. After 1h in the incubator at 37ºC, PBS solution was flowed through the same inlet for 2 minutes at a flow rate of 50 µL/min to wash the device. The device was stored at 4 ºC until the inoculation day. The coating was repeated at inoculation day.

II.8.3. HLCs inoculation and hepatocyte-chip operation

A concentration of 1 million cells/mL was resuspended in DM with 5% FBS and 20 µM of 5-AZA. Device inoculation was performed by flowing 5 µL/min for 2 minutes through the inlet **a** (Figure 3b), then 10 µL/min during 4 minutes through the same inlet, and, finally, 10 µL/min during 1 minute through the inlets **b**, **c**, **d**, and **e** (Figure 3b), which gave an inoculum of, approximately, 90000 cells/cm^2. After 1 h, medium was flowed at a rate of 0.2 µL/min. Cryopreserved HLCs were inoculated on D20 of differentiation into the hepatocyte's chamber by following a similar protocol.

In the final operation set-up (Figure 5), a syringe filled with culture medium was poured on the syringe pump, the metallic end of the tube plugged in the top inlet of the device. The inlets **a**, **b**, **c**, **d**, and **e** (Figure 3b) were plugged with closed metallic plugs, as well as the inlets created to close the communication to the culture medium chamber. The outlet was plugged with tube and an Eppendorf was attached to the other end.

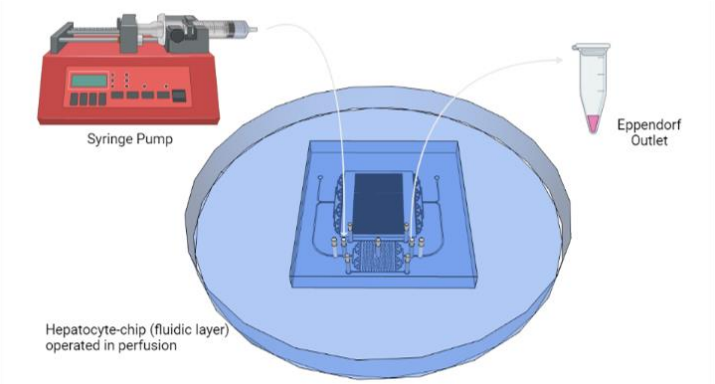

Figure 5- Scheme of the final perfusion set-up.

II.9. Valves actuation

To control the single valves (Figure 4a, valves 1, 2, 3 and 4), a mechanical pressure regulator (SMC Precision Regulator IR2010-F02, Orange Coast Pneumatics Inc.) connected to an array of normally closed solenoid valves (SMC SY114-5MZ-Q, Orange Coast Pneumatics Inc.) was used. First, the valve channel was filled with water. Accordingly, a piece of BTPE 60 tube was filled with DI water and plugged into the valve's inlet. In the other extremity, the tube was attached to a tubing coupler (SMC TU0425 polyurethane tubes, Orange Coast Pneumatics, Inc., Japan) that was coupled to the solenoid valve. The air pressure regulator was adjusted to 100 Pa until the channel was completely filled of water. To close the fluidic channel, the air pressure inside the valve channel was increased. To open the fluidic channel, the pressure of the regulator was decreased.

The pump (Figure 3a, pump 5) control was done using a teensy circuit board (Teensy 3.5, PJRC, USA) that was connected to the array of solenoid valves, and to the computer. The teensy circuit was supplied by a 24 V power source (HP Hewlett Packard E3612A DC Power Supply, USA).

II.10. Urea quantification

Urea was quantified in cell culture supernatants using a colorimetric urea kit (Urea Assay Kit, Abnova, Taiwan). The absorbance was measured at 520 nm in a microplate reader (SPECTROStar Omega, BMG Labtech, Germany). Data are presented as the rate of production $\mu g/10^6$ cells.h.

II.11. Statistical analysis

The results are presented as Average ± SEM. The urea and albumin quantifications were analyzed with two-way ANOVA with GraphPad Prism. A threshold of $p < 0.05$ was considered statistically significant.

III. Results and discussion

III.1. PS culture surface improved HLCs maintenance inside microfluidic devices

The first parameter to be optimized was the culture surface. From a biological point of view, it would be preferable to seal the devices against PS since the hepatic differentiation protocol herein pursued is performed normally using PS as a culture surface. Indeed, this culture surface is already optimized for the culturing of this cell type, and PS is the most widely used thermoplastic for laboratory cultureware having provided validated research conclusions regarding cell behavior and function throughout decades [28]. However, from a microfluidic point of view, a PDMS surface would be advantageous because it facilitates microfluidic valve control to allow fluid recirculation. Accordingly, initial tests were made to evaluate the adaptation of the HLCs in PS and PDMS culture surfaces in order to choose the optimum one to seal the device against. Two different experimental microfluidic devices, A (height of 0.1 mm and culture surface of 10 x 10 mm) and B (height of 0.1 mm and constituted by two chambers in a diamond-like shape, connected by 1 mm channels, with a culture surface of 12 x 4 mm), that were designed for cell culturing were used in this approach.

The devices were sealed against PS or PDMS. A coating of commercial collagen type I diluted with acetic acid was used since it was previously demonstrated to produce better results regarding the HLCs culturing inside commercially available microfluidic devices sealed against glass. HLCs were inoculated inside the devices on their D17 of differentiation. After cell adherence to the culture surface, the medium was then perfused into each device, introducing a unidirectional flow throughout the chamber.

The results show that, even though the cell's adhesion was not fully achieved in neither of the surfaces, the cells demonstrated a better adaptation in the device sealed against polystyrene (MD 1) since they were maintained in the chip longer than the cells from the chips sealed against PDMS (MD 2). On the day after the inoculation (day 1), the cells from MD 2 detached from the PDMS (Figure 6d). While, on the same day, the cells from MD 1 were still adherent to the PS (Figure 6c). However, three days after inoculation, the HLCs from the PS surface device started to detach (Figure 6e), which was believed to be due to the not yet optimized collagen coating and inoculum.

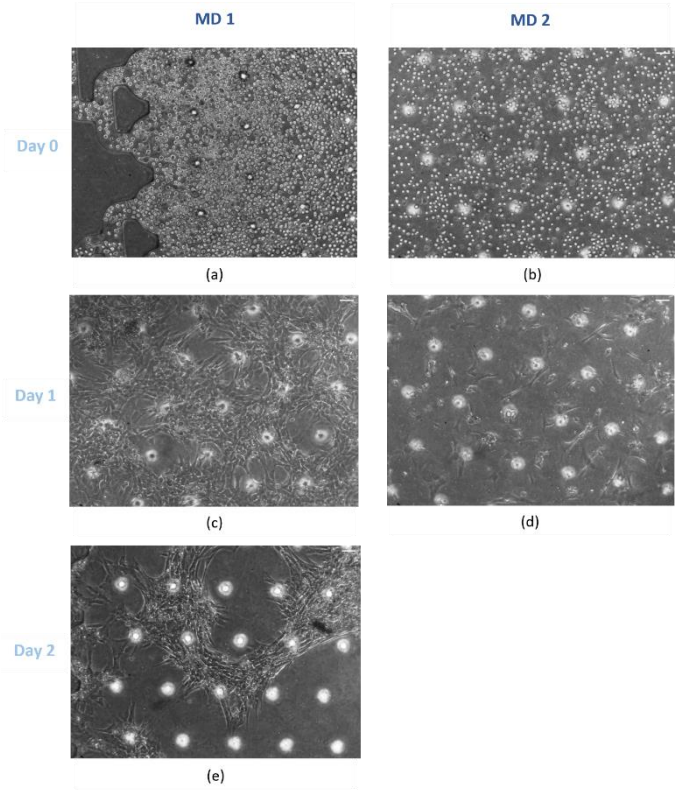

Figure 6- Cell's aspect, from day 0 to day 2, when cultured on PS (MD 1) and PDMS (MD 2) surfaces inside microfluidic devices. (a) and (b) cell's dispersion after being inoculated in the devices (day 0). (c) and (d) cell adhesion in PS and PDMS, respectively, one day after the cell's insertion (day 1). (e) HLCs on their second day (day 2) in the device sealed against PS. Scale bar = 100 µm.

III.2. Commercial collagen diluted with PBS provided better HLCs attachment to the PS culture surface

To enable a better attachment of the HLCs in the microfluidic devices sealed against PS, the coating was optimized. Commercial type I collagen was demonstrated to provide better coating results in commercially available microfluidic devices sealed against glass. Furthermore, the commercial collagen is purer and enables the development of standard coating methods in comparison with rat-tail collagen produced in the laboratory. Accordingly, only commercial collagen was chosen to test two different coating solutions, namely, commercial type I collagen diluted in acetic acid, and commercial type I collagen diluted in PBS. In general, PBS, as a collagen solvent, enables a better cell attachment to PS culture surfaces since it forms a more robust coating. However, because PBS is more viscous

than the acetic acid, may form clogs inside the microfluidic device once it solidifies, which may obstruct the chamber.

To test the two different coating conditions two experimental devices were used. In both, the collagen solution was inserted through the center access holes, for 2 min at 10 µL/min, to ensure that it was distributed equally throughout the chips. A concentration of 0.2 mg/mL in the two different collagen solutions was used, as it had already been optimized in the protocol. It is possible to notice a significant distinction in HLCs' adhesion on the two coatings. Indeed, one day after inoculation (day 1), the cells from MD 1 were confluent, adherent, and showed their typical polygonal shape (Figure 7c). On contrary, the cells from MD 2 were still rounded and detached from the coating surface (Figure 7d). Hence, the results indicate that HLCs had a better attachment in the chip coated with collagen diluted with PBS (Figure 7c) than in the device coated with collagen diluted with acetic acid (Figure 7d). Consequently, type I collagen diluted in PBS was chosen as the coating solution for the microfluidic devices.

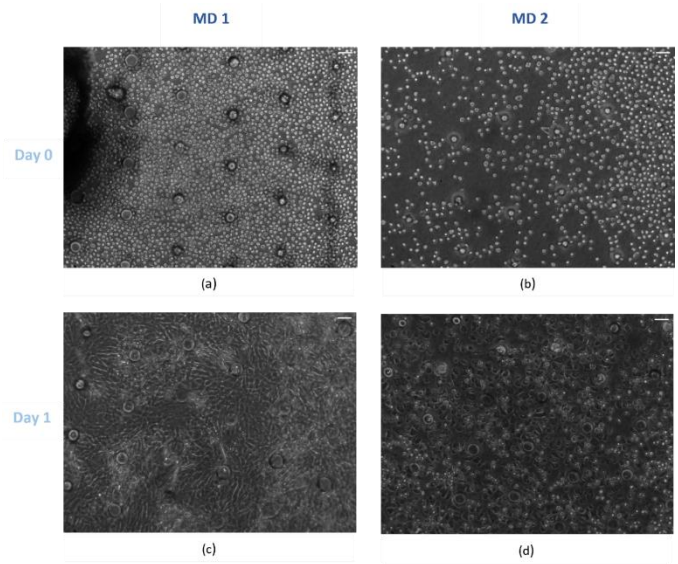

Figure 7- Cell's behavior when seeded on a PS culture surface coated with type I collage diluted with PBS (MD 1) and with acetic acid (MD 2). (a) and (b) cell's dispersion after being inoculated in the devices (day 0). HLCs, after one day of inoculation (day 1), on a surface coated using PBS (c) and acetic acid (d) are also presented. Scale bar = 100 µm.

Even though MD 1 fulfills the chosen condition, in this chip, the HLCs start to detach from the surface and lose their polygonal shape during the culturing. To avoid this problem, it was decided to perform the coating twice before cell inoculation to ensure cells' adhesion and morphology throughout the culture period.

The next step was to evaluate how much time was needed for the whole coating solution to cover the entire cell's chamber of the hepatocyte-chip once establishing a constant flow rate. It was concluded that 2 minutes at a flow rate of 50 µL/min was sufficient to fill the hepatocyte's chamber.

III.3. Right and left channels on the hepatocyte's chamber allowed better cell distribution into the sides

The next parameter to be optimized was the chip design, in particular, the hepatocyte's chamber. To maintain HLCs in culture it is required to achieve 100% confluency on the culture surface [29]. From the devices used previously, it was verified that device A, in comparison with each chamber of device B, demonstrated to have an architecture that was able to homogeneously disperse the cells throughout the chamber, providing better cell confluency and arrangement. This happened because device A has a square shape, meaning that, when inserting the HLCs through the center, the cells spread equally in all directions, ensuring a homogeneous and confluent surface. This is adequate since the cells enter the chamber in a radial direction. On the other hand, each chamber of device B has a high length-to-width ratio. Therefore, when inoculating the cells through the center inlet, there was a higher cell concentration in the right and left sides than in the top and bottom of the chamber. Inoculation through the top and bottom inlets was also attempted. However, the center part of the chamber will have fewer cells while the triangular parts near the top and bottom inlets will have high cell accumulation. Moreover, another advantage verified in device A was the presence of dispensers, which ensured that the culture medium is equally flowed throughout the culture area. Therefore, considering all these aspects, the cell's chamber of the hepatocyte-chip was designed to have a square shape with similar culture surface dimensions to device A (10 x 9 mm) and also to have two dispensers, one on the top and the other on the bottom to guarantee the unidirectional flow. The height of the device was the same as devices A and B since it was shown to be appropriate for HLCs culturing. In addition, several micropillars to ensure that the chamber does not collapse were distributed throughout the surface, except in the middle where the space necessary for an inlet to perform both the surface coating and HLCs' inoculation was created.

Cell insertion was tested to evaluate the efficacy of the designed hepatocyte (Figure 8a) chamber regarding cell distribution and seeding. It was verified that the cells were not homogeneously dispersed near the right and left sides of the chamber (Figure 8b). This happened because, when inserting the cells through the center inlet, they will tend to circulate towards the top and bottom inlets, as they are the only connection to the outside and, therefore, the ways that offer less resistance to the flow. To solve this problem, two side channels were added (Figure 8c). At each end of both channels, an access hole was placed to diminish the flow resistance to these parts of the cell's chamber. The addition of the side channels considerably improved the dispersion of the cells towards these specific zones (Figure 8d).

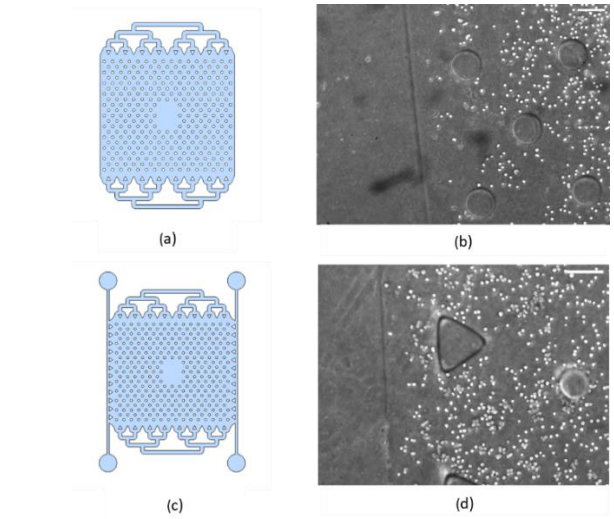

Figure 8- Comparison between cell dispersion in the chambers without (a) and with (c) the addition of the side channels. (b) and (d) the cell's disposition in one of the sides of the designed chambers (a) and (c), respectively. Scale bar = 200 µm.

III.4. HLCs could be homogeneously distributed into the hepatocyte's chamber

Inserting HLCs from a solution with 1 million cells/mL provided a good distribution and concentration of cells throughout the culture surface. Starting cell inoculation with a flow rate of 5 µL/min for 2 minutes allowed a slow radial cell's entrance, ensuring a controlled diffusion (Figure 9a). In the second step, the flow rate was increased to 10 µL/min for 2 minutes while the tube was being rotated in intervals of 30 seconds to the sides of the chamber (Figure 9b). By elevating the flow rate, the cells already inside the device were pushed to furthest chamber zones, particularly to the side parts. The third step included more 10 µL/min flow rate for 2 minutes with the tube being rotated towards the chamber corners in intervals of 30 seconds (Figure 9c). This was required to increase the concentration of cells in the corners. Through this protocol, confluency was not achieved, especially on the right and left sides. Since, in the context of maintaining hepatocytes in culture, it is very important to ensure high cell-to-cell contact to reach optimum confluency, it was necessary to add another step to the inoculation protocol [29]. Therefore, this step consisted in inserting the cells through the inlets **b**, **c**, **d**, and **e** (Figure 3b) for 1 minute each (Figure 9d).

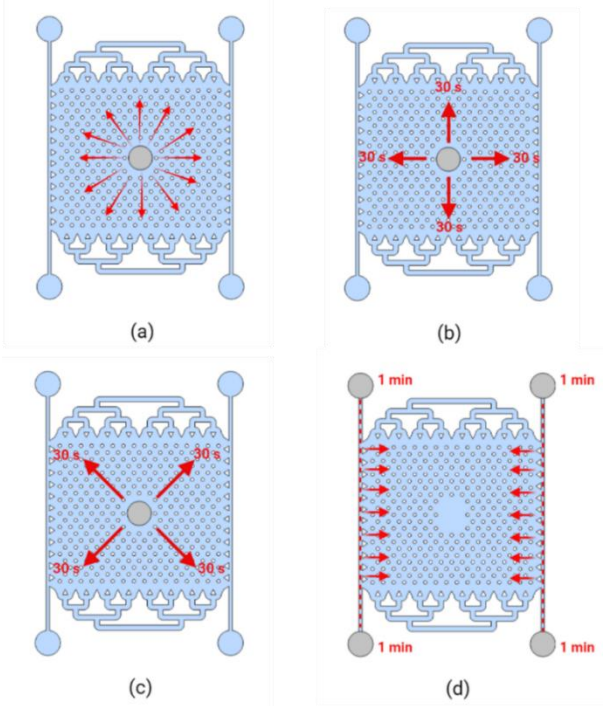

Figure 9- Optimized inoculation steps.

III.5. HLCs could be maintained in perfusion for more than one week in the designed hepatocyte's chamber

Characterization of HLCs in the hepatocyte's culture chamber was performed. Herein, the perfusion hepatocyte-chip structure was used. It was possible to maintain in culture the HLCs into the device for 17 days by starting the inoculation on their D17 (day 0 in the MD) of differentiation and ending on D34 (day 17 in the MD). After inoculation (day 0), the HLCs looked well dispersed through the entire chamber (Figure 10). It is also possible to verify that after 1h in the incubator the cells were adherent. Moreover, throughout the culturing days, HLCs present a tissue-like aspect, exhibiting their typical polygonal shape, throughout the whole chamber including the dispensers and side channels (as shown in Figure 10 on days 1, 4, 7, and 10). This confirms the efficacy of the side channels and demonstrates that the coating is being well performed as it is reaching these furthest chamber zones. HLC morphology was maintained throughout the whole culture.

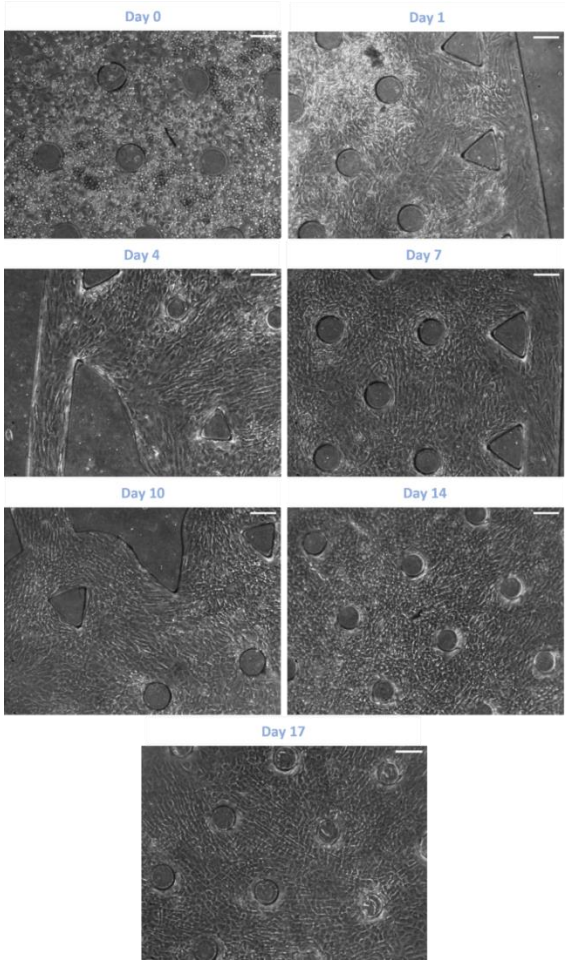

Figure 10- Maintenance of HLCs inside the designed cell chamber for 17 days. In each image, it is represented the cell's aspect in different zones of the chamber in some days (0, 1, 4, 7, 10, 14, and 17) after inoculation. Scale bar = 200 µm.

To evaluate the HLCs phenotype throughout the culture time inside the microfluidic device, urea production was accessed from the cell's supernatant. Urea was measured in HLCs maintained for 4 and 7 days in the device. Urea production from HLCs in microfluidic devices was compared with the one produced by HLCs in 2D plates, undifferentiated hnMSCs, HepG2, a regularly used hepatic cell line, and hpHep, the gold standard cell source for hepatic *in vitro* models. In Figure 11, we can observe that after 7 days in culture, urea production by HLCs in the chip is similar to that of HepG2 and higher than HLCs in plates (p <0.001). It is also noticeable that from day 4 to day 7, urea production increases in the microfluidic device, meaning that cells improve their phenotype and metabolic functions during the culture time inside the chip.

Cryopreserved HLC culture was also tested in the hepatocyte-chip and plates, and the amount of urea secreted was accessed. Those cells are HLCs that were cryopreserved on their D17 of differentiation. After being unfrozen, they were seeded on 24-well plates until D20. On D20, their inoculation on the hepatocyte's chamber and other culture plates was performed. Cryopreserved cells are ready-to-use cells since they already acquire some maturation level before being preserved. Therefore, cryopreserved HLCs are rapidly available. However, cryopreserved cell's phenotype is still poor

because the techniques used to cryopreserve are aggressive for cells and may cause loss of functions [30].

In Figure 12 it is possible to observe the results regarding the urea production of cryopreserved HLCs achieved in microfluidic and plate cultures. In comparison with freshly differentiated HLCs cultured in devices, the cryopreserved HLCs in devices were able to produce less urea. Nevertheless, the urea secreted in cryopreserved HLCs seeded in devices is higher than the one present in the plate's supernatant, showing the potential of microscale cultures in comparison to the typical monolayer cultures in improving hepatic functions.

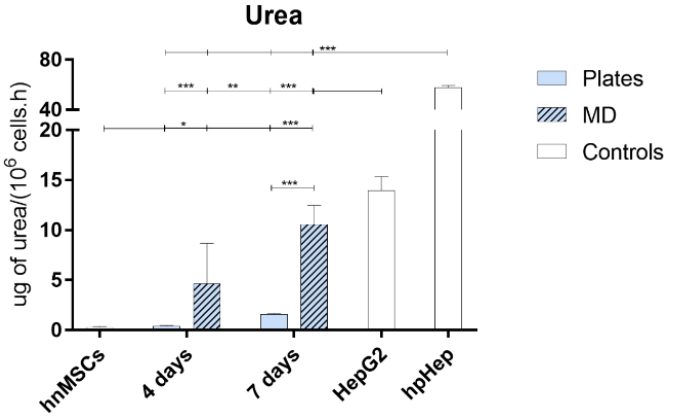

Figure 11- Urea production 4 and 7 days after the inoculation of HLCs into the microfluidic device and plates. Undifferentiated hnMSCs are the negative control. HepG2 and hpHep are positive controls. *, **, *** Significantly differs among the controls with $p < 0.05$, $p < 0.01$ and $p < 0.001$, respectively.

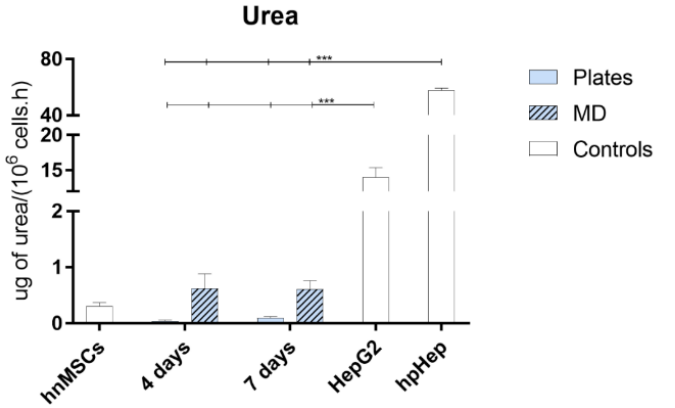

Figure 12- Urea production 4 and 7 days after inoculation of cryopreserved HLCs into the microfluidic device and plates. Undifferentiated hnMSCs are the negative control. HepG2 and hpHep are positive controls. *, **, *** Significantly differs among the controls with $p < 0.05$, $p < 0.01$ and $p < 0.001$, respectively.

III.6. Pneumatic valves allow complete fluidic channel closure

With the view to use the control layer valves in the culturing of HLCs in the designed chip to provide medium recirculation, the control and fluidic layers of the hepatocyte-chip were combined (recirculation hepatocyte-chip structure) and tests were done to investigate if the dimensions of the valves, fluidic channel, and PDMS membrane placed in between were suited for the complete fluidic channel closure, and therefore, for the correct pneumatic control.

Al the single valves (Figure 4a, valves 1, 2, 3, or 4) actuation was individually tested. A dye solution was flowed through the fluidic channel that was underneath the valve to be tested, to simulate the culture medium Air pressure was continuously applied to the valve channel by adjusting the regulator until the complete fluidic channel closure was visualized and checked under the microscope. Figure 13c demonstrates that the valve is able to completely close the underneath channel, validating the pneumatic valve's operation. However, that was only possible if high pressures were applied, between 350 Pa and 400 Pa, which can lead to the unsealing of the layers if long periods of actuation are done.

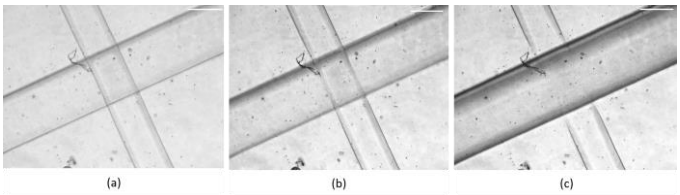

Figure 13- Valve operation with the increase of air pressure. The valve channel is above and the fluidic layer channel is underneath. The air pressure inside the valve channel is increasing from (a) to (c). In (c) the valve is being actuated with 400 Pa and the fluidic channel is completely closed. Scale bar = 300 µm.

The pump (Figure 4a, 5) was also tested to verify if fluid recirculation throughout the hepatocyte's chamber was possible. When increasing the air pressure regulator close to 400 Pa, each valve was able to close (valve actuated) and open (valve non-actuated) the fluidic channel while the teensy code was being employed, allowing the pump operation. However, the unsealing of the fluidic and control layers occurred minutes after the starting of the pump operation. Indeed, the consecutively application of high pressures to each valve channel and the sudden depressurization led to the rapid device failure.

IV. Conclusions and Future Perspectives

Perfusion experiments using the HLCs chamber were first attempt with the aim to adapt the cells into the chip. It was concluded that a PS surface provided better HLCs attachment. A collagen type I diluted in PBS demonstrated better results regarding HLCs adhesion and maintenance. The firstly designed hepatocyte's chamber did not provide optimum cell dispersion and confluency, consequently, a new chamber was designed and fabricated including side channels. Cells' inoculation was optimized by achieving an automatized protocol that not only ensured 100% cell confluency. HLCs were successfully maintained inside the chip during at least one week in perfusion, having demonstrated a polygonal morphology and a tissue-like aspect throughout the culturing. HLCs cultured in the device produce more urea than HLCs in plates, and that this production increased. Cryopreserved HLCs seeded in the chip also demonstrated superior urea production than the ones from the plates, which corroborates, once again, the potential of microscale cultures.

Embed pneumatic valves into the HLCs culture with the view to automatize the culture process by including culture medium recirculation was also attempted. From the performed valve tests, it can be concluded that the valves were capable of closing the fluidic channel through high actuation pressures, which led to the unsealing of the layers when the pump was operating. Therefore, future valve optimizations will be required.

Since the number of cells cultured in the chip is much lower comparing with macroscale cultures, some traditional laboratory protocols cannot be employed, such as qPCR and western blot. Accordingly, adapting these protocols to the microfluidic device

could be done in the future using, for instance, imaging-based assays, such as immunofluorescence.

The use of microfluidic devices to provide *in vitro* human models is currently in vogue, however, there is still a lack of experience in the use of these chips in biological applications because it is required expertise in both cell culturing and microfluidic design and fabrication. Therefore, it is often required the cooperation of different teams to be well succeeded in the conception of physiologically relevant models. This work provides both, a biological and a microtechnological perspective regarding the conception of a hepatic model for *in vitro* research, which helps to close the gap between these two fields of study. Furthermore, because microfluidics' cell cultures are yet a novel method, there are not so many studies of hepatic models in chips, which makes these a trial-and-error approach, as we proceed in this work. Here, it was presented a set of optimizations that are thought to be useful for the future researchers of this field of study.

V. Acknoledgements

This document was written and made publicly available as an institutional academic requirement and as a part of the evaluation of the MSc thesis in Biomedical Engineering of the author at Instituto Superior Técnico.

The work described herein was performed at the INESC-MN, Instituto de Engenharia de Sistemas e Computadores - Microsistemas e Microtecnologias, University of Lisbon (Lisbon, Portugal), and at iMed.ULisboa, Instituto de Investigação do Medicamento, University of Lisbon (Lisbon, Portugal), during the period March-October 2021, under the supervision of Dr. João Pedro Conde and Dr. Joana Miranda, respectively.

VI. References

1. Liver: Anatomy and Functions | Johns Hopkins Medicine (Accessed: 29/03/2021). https://www.hopkinsmedicine.org/health/conditions-and-diseases/liver-anatomy-and-functions.
2. Kalra, A. & Tuma, F. *Physiology, Liver*. *StatPearls* (StatPearls Publishing, 2018).
3. The Liver - Lobes - Ligaments - Vasculature - TeachMeAnatomy (Accessed: 29/03/2021). https://teachmeanatomy.info/abdomen/viscera/liver/.
4. Wang, L. & Boyer, J. L. The Maintenance and Generation of Membrane Polarity in Hepatocytes. *Hepatology* vol. 39 892–899 (2004).
5. Nguyen-Lefebvre, A. T. & Horuzsko, A. Kupffer Cell Metabolism and Function. *J. Enzymol. Metab.* **1**, 1-101 (2015).
6. Jager, J., Aparicio-Vergara, M. & Aouadi, M. Liver innate immune cells and insulin resistance: the multiple facets of Kupffer cells. *J. Intern. Med.* **280**, 209–220 (2016).
7. Chiang, J. *Liver Physiology: MetaboLism and Detoxification*. *Pathobiology of Human Disease: A Dynamic Encyclopedia of Disease Mechanisms* (Elsevier Inc., 2014).
8. Rui, L. Energy metabolism in the liver. *Comprehensive Physiology* vol. 4 177–197 (2014).
9. The Liver | Boundless Anatomy and Physiology (Accessed: 29/03/2021). https://courses.lumenlearning.com/boundless-ap/chapter/the-liver/.
10. E, B., AJ, M. & G, M. Insulin resistance: a metabolic pathway to chronic liver disease. *Hepatology* **42**, 987–1000 (2005).
11. Rakhra, V., Galappaththy, S. L., Bulchandani, S. & Cabandugama, P. K. Obesity and the Western Diet: How We Got Here. *Mo. Med.* **117**, 536 (2020).
12. Al-Goblan, A. S., Al-Alfi, M. A. & Khan, M. Z. Mechanism linking diabetes mellitus and obesity. *Diabetes, Metab. Syndr. Obes. Targets Ther.* **7**, 587–591 (2014).
13. Leclercq, I. A., Da Silva Morais, A., Schroyen, B., Van Hul, N. & Geerts, A. Insulin resistance in hepatocytes and sinusoidal liver cells: Mechanisms and consequences. *J. Hepatol.* **47**, 142–156 (2007).
14. Kitade, H., Chen, G., Ni, Y. & Ota, T. Nonalcoholic Fatty Liver Disease and Insulin Resistance: New Insights and Potential New Treatments. *Nutrients* **9**, 387 (2017).
15. Zeilinger, K., Freyer, N., Damm, G., Seehofer, D. & Knöspel, F. Cell sources for in vitro human liver cell culture models. *Exp. Biol. Med.* **241**, 1684 (2016).
16. Iwatani, S. *et al.* Isolation and characterization of human umbilical cord-derived mesenchymal stem cells from preterm and term infants. *J. Vis. Exp.* **2019**, e58806 (2019).
17. Cipriano, M. *et al.* The role of epigenetic modifiers in extended cultures of functional hepatocyte-like cells derived from human neonatal mesenchymal stem cells. *Arch. Toxicol.* **91**, 2469–2489 (2017).
18. Whitesides, G. M. The origins and the future of microfluidics. *Nature* **442**, 368–373 (2006).
19. Gale, B. K. *et al.* A review of current methods in microfluidic device fabrication and future commercialization prospects. *Inventions* **3**, 60 (2018).
20. Microfluidics: A general overview of microfluidics - Elveflow (Accessed: 15/06/2021). https://www.elveflow.com/microfluidic-reviews/general-microfluidics/a-general-overview-of-microfluidics/.
21. Convery, N. & Gadegaard, N. 30 Years of Microfluidics. *Micro Nano Eng.* **2**, 76–91 (2019).
22. Serras, A. S. *et al.* A Critical Perspective on 3D Liver Models for Drug Metabolism and Toxicology Studies. *Front. Cell Dev. Biol.* **9**, 1–30 (2021).
23. Ziółkowska, K., Kwapiszewski, R. & Brzózka, Z. Microfluidic devices as tools for mimicking the in vivo environment. *New J. Chem.* **35**, 979–990 (2011).
24. Xie, X. & Livermore, C. Liver-on-a-Chip Models of Fatty Liver Disease. (2020).
25. Rajan, N., Habermehl, J., Coté, M. F., Doillon, C. J. & Mantovani, D. Preparation of ready-to-use, storable and reconstituted type I collagen from rat tail tendon for tissue engineering applications. *Nat. Protoc.* **1**, 2753–2758 (2007).
26. Martins, J. P. *et al.* Towards an advanced therapy medicinal product based on mesenchymal stromal cells isolated from the umbilical cord tissue: Quality and safety data. *Stem Cell Res. Ther.* **5**, 1–15 (2014).
27. Santos, J. M. *et al.* Three-dimensional spheroid cell culture of umbilical cord tissue-derived mesenchymal stromal cells leads to enhanced paracrine induction of wound healing. *Stem Cell Res. Ther.* **6**, 1–19 (2015).
28. E, B., EW, Y. & D, B. Engineers are from PDMS-land, Biologists are from Polystyrenia. *Lab Chip* **12**, 1224–1237 (2012).
29. Ben-Ze'ev, A., Robinson, G. S., Bucher, N. L. & Farmer, S. R. Cell-cell and cell-matrix interactions differentially regulate the expression of hepatic and cytoskeletal genes in primary cultures of rat hepatocytes. *Proc. Natl. Acad. Sci. U. S. A.* **85**, 2161 (1988).
30. Stéphenne, X., Najimi, M. & Sokal, E. M. Hepatocyte cryopreservation: Is it time to change the strategy? *World J. Gastroenterol.* **16**, 1 (2010).